

# Functional Polymers for Colloidal Application. VI. Syntheses and Dispersing Ability of Lipomodified Naphthalenesulfonate Formaldehyde Condensates

PING-LIN KUO,\* JIAAU-SHAHNG LIN, and BIH-SHIUH WEY

Department of Chemical Engineering, National Cheng Kung University, Tainan, Taiwan 70101, Republic of China

## SYNOPSIS

Butyl-substituted naphthalenesulfonate formaldehyde condensates (C4NSF) with different molecular weights were synthesized. The structures were confirmed by NMR in terms of the appearance of the signal at  $\delta = 3.3\text{--}4.0$  ppm, and the molecular weights of the synthesized C4NSFs were compared by gel permeation chromatography (GPC). C4NSFs used as dispersants were compared to unmodified naphthalenesulfonate formaldehyde condensates (NSF) in their ability to disperse nonpolar particles (carbon black) and polar particles ( $\text{TiO}_2$ ) in water. Their dispersing ability was evaluated by both a viscosity method and a microscopy method. For dispersing carbon black in water, it was found that using C4NSFs as dispersing agents results in a lower viscosity, a lower yield value by the viscosity method, and a more homogeneous dispersion of particles as determined by microscopy. These results indicate that the butyl group enhances the dispersing ability of C4NSF. The effect of the butyl group on the dispersing ability of C4NSF was interpreted by the results of the measured adsorption amount that was also enhanced by the existence of the butyl group. For dispersing  $\text{TiO}_2$  in water, C4NSF results in a higher viscosity and a higher adsorption amount of the dispersed system than NSF. These phenomena were interpreted in terms of the hydrophobic interaction between the butyl groups and the bridging effect. © 1993 John Wiley & Sons, Inc.

## INTRODUCTION

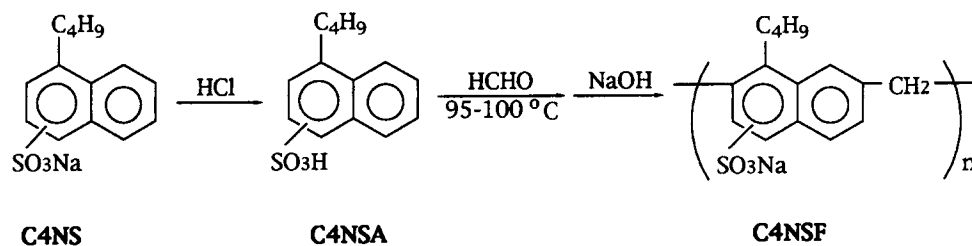
Dispersing technology is widely used both in conventional industries (such as coatings, pigments, and dyes),<sup>1-5</sup> and high-tech industries (such as magnetic slurring and photocopying).<sup>6</sup> In order to acquire a stable dispersion, a dispersant is usually added to help suspend solid particles in liquid. The main function of the dispersant is to provide the particles with an electrostatic barrier<sup>7</sup> and/or with steric<sup>8</sup> hindrance to prevent coagulation. In addition to surfactants and polymers such as polycarboxylates, naphthalenesulfonate formaldehyde condensates (NSF) are usually used as industrial dispersants.

To disperse particles effectively, dispersants have to adsorb on the surface of particles efficiently. Therefore, the dispersing ability of a dispersant is

strongly affected by its structure that influences its adsorption behavior. Because of the strong interaction of NSF with polar and nonpolar surfaces, NSFs have been widely used for the dispersion of dyes, coal, and cement in aqueous systems.<sup>9-16</sup> For dispersing nonpolar particles such as coal, the adsorption of NSF on nonpolar surfaces mainly arises from the interaction between the polarizable naphthalene ring and the nonpolar surface.<sup>17,18</sup> If NSF is modified with an alkyl group in each unit of the condensate, then the hydrophobicity of NSF is increased, and the adsorption onto the nonpolar surface will be promoted. Thus, its dispersing ability will be influenced by the introduction of alkyl groups to the naphthalene rings.

In this study, butyl-substituted naphthalenesulfonic acid was condensed with formaldehyde to prepare a butyl-substituted NSF (referred as C4NSF) shown in Scheme 1, which was used to disperse carbon black and  $\text{TiO}_2$ , both in aqueous solution. The dispersing ability of C4NSF was assessed by rheo-

\* To whom correspondence should be addressed.



**Scheme 1** Synthesis of C4NSF from C4NS.

logical methods and by electron microscopy, and interpreted in terms of the adsorption measurements. The experimental results for C4NSF are compared with those for NSF.

## EXPERIMENTAL

### Materials

Sellogen-W (Henkel, a butyl-substituted naphthalenesulfonate) was used in its monomeric form after being converted to its acid type (C4NSA) by precipitating it in a 50% HCl solution. Formaldehyde (Merck, 37 wt %, EP Grade) was used without further purification. A pure acrylic latex (External 1180, 50% solid, External Chemical Co.), TiO<sub>2</sub> (Dupont R-900, with surface area 57.6 m<sup>2</sup>/g, density 4.0 g/cm<sup>3</sup>), and carbon black (Cabot N660, with nitride absorbed surface area 35 ± 7 m<sup>2</sup>/g, pour density 425 ± 30 kg/m<sup>3</sup>) were used as supplied. The water used in these experiments is ion-exchanged and distilled, with a pH between 6.8–7.2, and conductivity of 4.4 × 10<sup>-6</sup> Ω<sup>-1</sup> m<sup>-1</sup>.

### Methods

#### Synthesis and Characterization of Condensates

*Synthesis of C4NSF (as Scheme 1).* Sellogen-W was precipitated in 50% HCl solution, and then dried and leached with acetone to obtain monomeric C4NS acid. In a four neck reaction kettle, C4NS acid (100 g) and formaldehyde (37%, 92 g) were well mixed and then a solution of H<sub>2</sub>SO<sub>4</sub> (35%, 52.7 g) was added as a catalyst. Condensation was carried at 95–100°C for 12 and 24 h, respectively. The longer time results in condensates of higher *M<sub>w</sub>* as discussed later in the text. Water was added to terminate the reaction and Ca(OH)<sub>2</sub> was added to precipitate out SO<sub>4</sub><sup>2-</sup> as CaSO<sub>4</sub>. The mixture was filtered, dried, and leached with acetone to obtain C4NSF (acid type). C4NSF sodium salts were obtained by adjusting to

pH 9.0 with NaOH and then drying in a vacuum oven.

*Characterization of Condensates.* C4NS and acid type C4NSF dissolved in D<sub>2</sub>O were characterized by H<sup>1</sup>-NMR (Bruker WP 100) (Fig. 1). For C4NS, the protons on the naphthalene ring appear at δ = 6.5–8.0 ppm, and those on butyl group appear at δ = 0.5–1.5 ppm. After reaction, the protons on the naphthalene ring and butyl group appear at similar field strength as C4NS; however, the methylene group between two naphthalene rings was found at δ = 3.0–4.0 ppm similar to an usual methylene proton.<sup>19,20</sup> Molecular weight distributions of C4NSF (sodium salts) obtained under different reaction conditions were compared by the GPC method<sup>21–23</sup> (Table I). Three GPC columns (Waters Ultrahydrogel-120, 250, 500, 30-cm length, 7.8-mm inner diameter, fully porous, highly crosslinked hydroxylated polymer as packing material) were combined in series for the measurements, and water (GPC grade) was used as the mobile phase.

#### Evaluation of the Dispersing Abilities of Condensates

The TiO<sub>2</sub>/water, and carbon black/water systems were prepared by using different condensates as dis-

**Table I** Reaction Time and GPC for the C4NSFs With Different Degrees of Polymerization

Sample Name	Reaction Time <sup>a</sup> (h)	Percentage of High <i>M<sub>w</sub></i> <sup>b</sup>	Elution Curve
H-C4NSF	24	57.1	Figure 2(a)
L-C4NSF	12	16.9	Figure 2(b)
C4NS	—	0	Figure 2(c)

<sup>a</sup> The molar ratio of HCHO/C4NSF was fixed at 3/1.

<sup>b</sup> The percentage of the peak area below the retention time of 15 min.

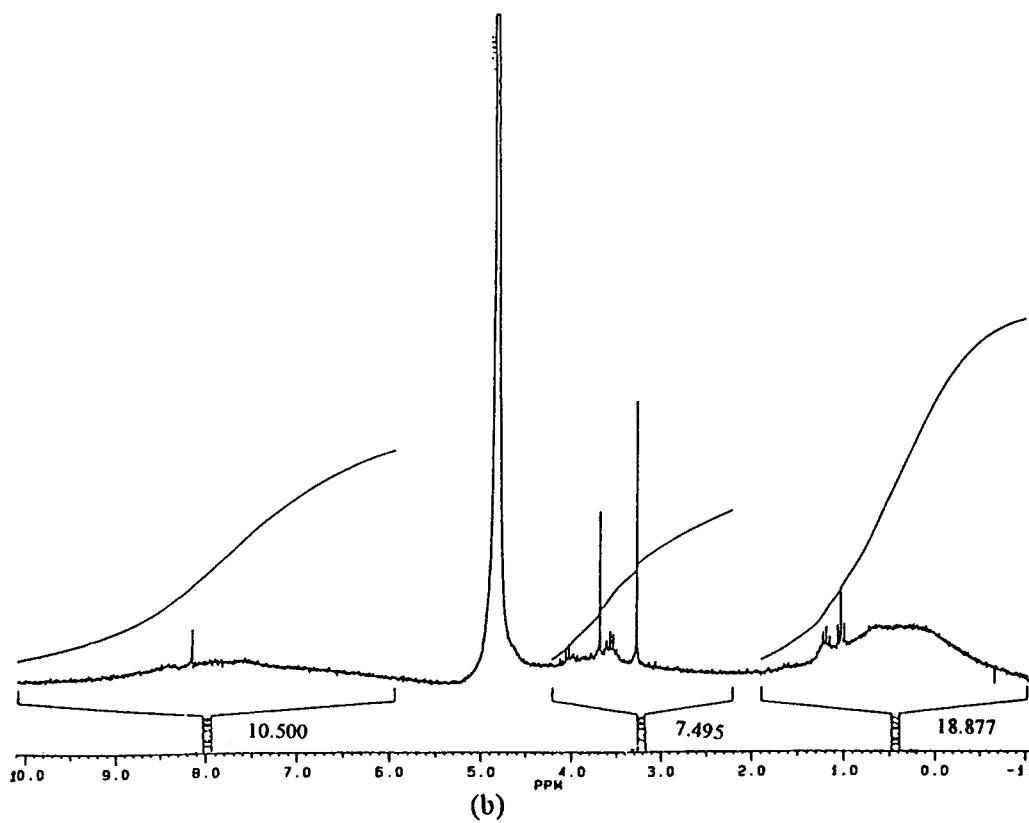
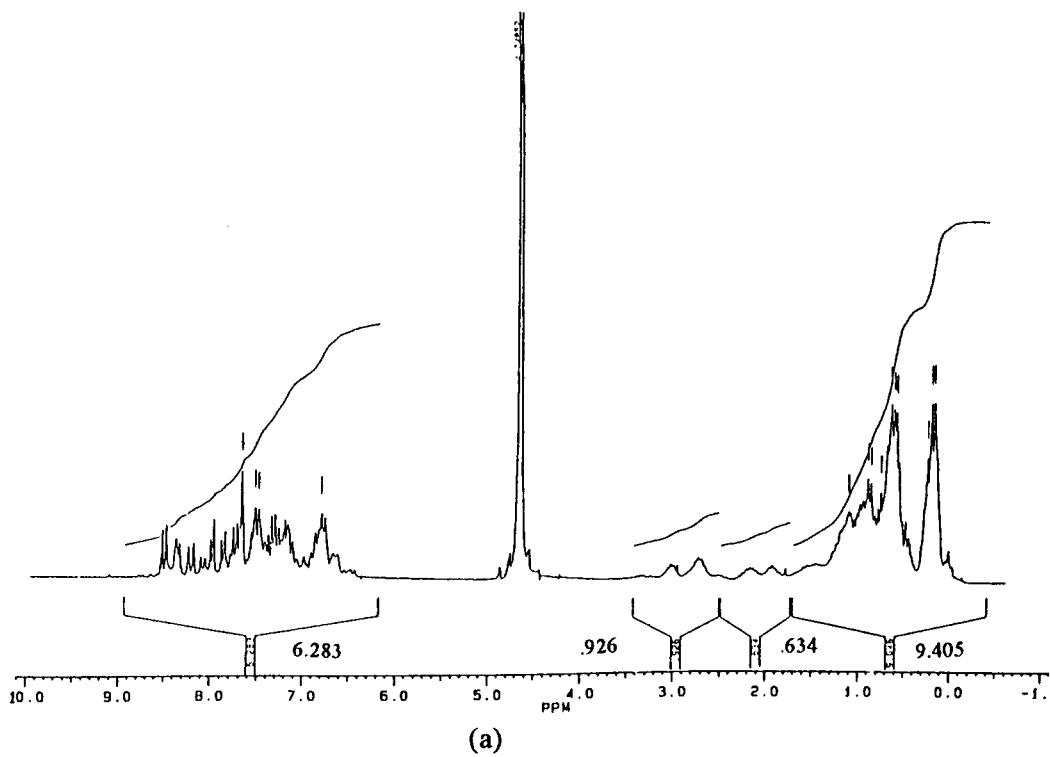


Figure 1 (a) NMR spectra of C4NS; (b) NMR spectra of C4NSF.

**Table II** Formulation for Dispersing Carbon Black and TiO<sub>2</sub> in Water

Material	Weight (g)	
	Carbon Black	TiO <sub>2</sub>
Carbon black	30	—
TiO <sub>2</sub>	—	50
Water	40	17
Latex	30	60
Dispersant	0–8% of carbon	0–8% of TiO <sub>2</sub>

persants. Table II shows the formulation used in these experiments. The dispersant was dissolved in water (40 g) and the latex (30 g) was added and mixed, then carbon black (30 g) and 1-mm diameter glass balls (150 g) were added. The mixture were stirred mechanically at 600 rpm for 60 min, and the temperature was maintained at 25°C. The mechanical stirrer was equipped with a 34-mm diameter paddle, i.e., the circular speed is 64.09 m/min. All the prepared pastes were assessed by the following methods:

**Rheological Method.** Using a rotating cylindrical viscometer (Brookfield DVII LVT), 10 mL of dispersion was put in the adapter with a SCS-31 spindle. The apparent viscosity (shear rate: 20.4 s<sup>-1</sup>) and yield value (using the Casson equation) were used as parameters to evaluate the dispersion ability of the above dispersants. All of the shear stress–shear rates were measured at 25°C.

**Scanning Electron Microscopy (SEM).** The dispersed paste (1 g) was used to coat (c.a. 25 μm of wet film thickness) on a thin copper plate. After drying (in the room for one day), a small piece of the paste (c.a. 4 mm × 4 mm) was cut and put on an aluminum sheet (20-mm diameter) and electro-deposited with a layer of gold. The surface of the film was observed by an SEM electron probe microanalyzer (Jeol TXA-840).

#### Characterization of the Adsorption of Condensate

The adsorption of the dispersants onto TiO<sub>2</sub> and carbon black surfaces was measured as follows. In a 50 mL bottle, 5 g of TiO<sub>2</sub> (or carbon black) was put into 50 mL of the prepared aqueous solution of dispersant with latex at a series of different dispersant concentrations. After shaking in a thermal bath (25°C, 300 rpm) for 48 h, the suspension was centrifuged by Dupont Sorvall RC-5B at 10,000 rpm

for 40 min at 25°C. The equilibrium concentrations of dispersants in the bulk phase were determined by UV absorption (Jasco 7800) at 232 nm in terms of an adsorption calibration curve.

## RESULTS AND DISCUSSION

Naphthalenesulfonate formaldehyde condensates were prepared by the sulfonation of naphthalene at 120–160°C followed by the condensation with formaldehyde (HCHO) at 95–100°C.<sup>9–12</sup> The reaction rate was influenced by the concentrations of HCHO, naphthalene sulfonate (NS), and H<sub>2</sub>SO<sub>4</sub> (as catalyst). The rate determining step is the methylation of NS, i.e., the reaction of the protonated HCHO with NS.<sup>24</sup> The butyl group is an electron-donating group so it favors the methylation of C4NS; however, the butyl group is bulky and may exhibit steric hindrance effects on the methylation of C4NS. Due to the influence of the butyl group in C4NS, the procedures used to synthesize C4NSF from C4NS in this study are modified from these used to synthesize NSF from NS. The main differences are to increase the time of condensation.

The formation of condensates can be characterized by NMR as well as GPC, i.e., C4NSF has the methylene peak at  $\delta = 3.3\text{--}4.0$  ppm as NSF<sup>19,20</sup> [Fig. 1(b)], which cannot be observed for C4NS (Fig. 1). The appearance of two peaks at  $\delta = 3.3\text{--}4.0$  ppm means the nonequivalent of the protons in different methylene groups, since on the naphthalene ring, the carbon attached to the methylene group can be neighbored with a carbon either substituted by a butyl group or not. However, the area ratio of the methylene protons to the aromatic protons of the naphthalene moiety cannot be used to accurately estimate the degree of polymerization of C4NSF ( $n$  value of C4NSF), since the ratio is not changed with the  $n$  value remarkably.

Conventional NSF is a condensate with the degree of polymerization of 2–10. Such a low molecular-weight polymer was qualitatively characterized by thin layer<sup>11</sup> or by GPC.<sup>23</sup> For either case, molecular weight was never calculated, but only the shape of molecular-weight distribution in GPC or the number of spots on thin-layer plate was shown. If the molecular weight of NSF is calculated by GPC based on the calibration standard of polyethylene glycol, the calculated molecular weight is tremendously high and does not make sense. Figure 2 shows the molecular-weight distribution of H-C4NSF and L-C4NSF compared with C4NS. Obviously, the area of the peaks appeared at lower elution time is sig-

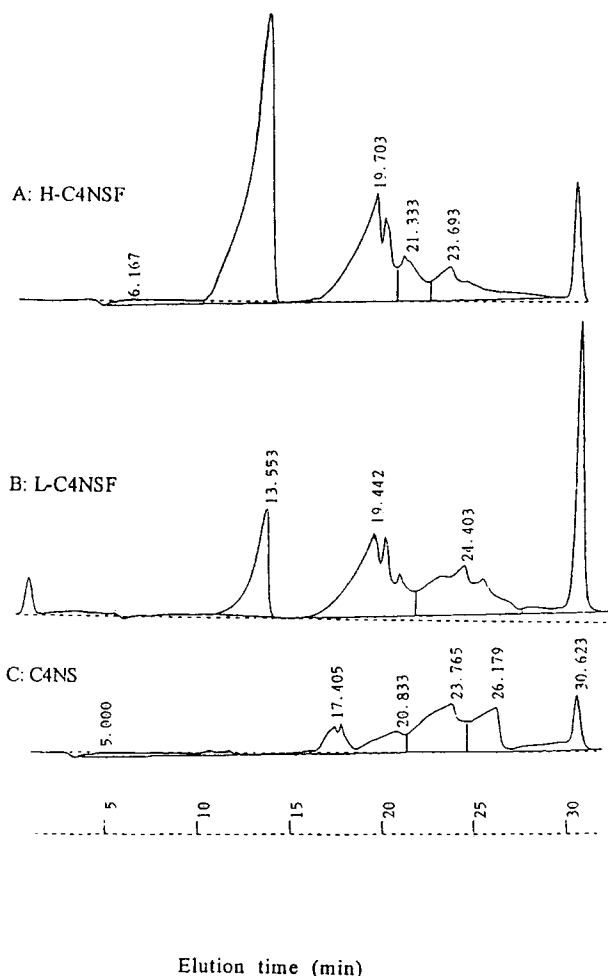


**Figure 2** GPC spectra of C4NS and of C4NSFs with high molecular weight (H-C4NSF), and low molecular weight (L-C4NSF).

nificantly higher for H-C4NSF than that for L-C4NSF, e.g., the peak area below 15 min is 57.1% for H-C4NSF compared with 16.9% for L-C4NSF (Table I). Since the reaction time is longer for H-C4NSF than L-C4NSF, the longer condensation time increases the degree of polymerization of the condensates. However, if the reaction time is too long, the C4NSF will become gel due to the occurrence of crosslinking between the aromatic rings of the C4NSF.

For a solution with low-solids content, the Einstein-Stokes equation<sup>25</sup> can be used to express the viscosity of the solution as a function of  $\eta_s$  (the viscosity of solvent) and the volume fraction of the solid. For a dispersing system with high solids content, the shear rate ( $\gamma$ ) and the shear stress ( $\tau$ ) have a functional relationship of  $\gamma = k\tau^n$ .<sup>25</sup> On a plot of  $\tau$  vs.  $\gamma$  of a plastic flow, the intercept and the

apparent viscosity ( $\tau/\gamma$ ) are useful parameters to estimate the extent of dispersion of a system. In this study, a Brookfield DVII LVT (a low shear-rate viscometer), with a spindle of SC4-34 was used to measure the  $\tau$  and the  $\gamma$  values.

For the test systems using C4NSF as a dispersant (e.g., C4NSF dispersing carbon black in water), the relation between  $\tau$  and  $\gamma$  at different dispersant concentrations is shown in Figure 3(a). Apparently,

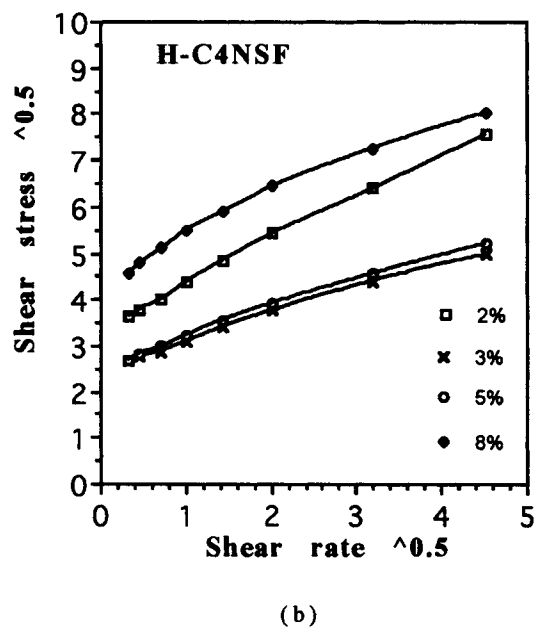
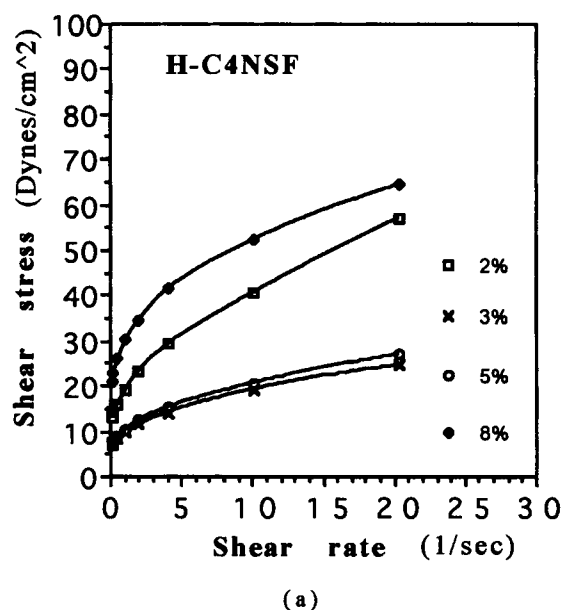


**Figure 3** The relation (a) between  $\tau$  and  $\gamma$ , and (b) between  $\tau^{1/2}$  and  $\gamma^{1/2}$  using H-C4NSF as a dispersant in the carbon black/ $H_2O$  system.

this dispersing system shows a plastic flow with a remarkable yield. The relationship between  $\tau$  and  $\gamma$  can also be expressed in terms of the Casson equation.<sup>1,26,27</sup>

$$\tau^{1/2} = \tau_0^{1/2} + \eta_{\infty}^{1/2} \gamma^{1/2}$$

where  $\eta_{\infty}$  is the apparent viscosity under an extremely high shear rate.  $\tau_0$  is the shear stress at a shear rate of near zero such that  $\tau_0$  is close to the value mentioned above. Thus, if the plot of Figure 3(a) is plotted in terms of  $\tau^{1/2}$  vs.  $\gamma^{1/2}$  [Fig. 3(b)], then the yield value can be acquired from Figure 3(b). As the concentration increases, the yield value decreases to a minimum at about 3 wt % and then increases again (Fig. 4). According to the definition for  $\tau_0$  in the Casson equation, the yield value is the minimum shear stress to break the flocs aggregates in a dispersing system. It is a parameter that indicates the interaction between the particles of flocs, such that the higher is the yield value, the stronger is the interaction between the particles. The results in Figure 3(b) imply that the interaction between particles decreases and then increases again as the dispersant concentration increases. Figure 4 shows the yield value as a function of dispersant concen-

tration for different type of dispersants (C4NS, NSF, and C4NSF with different degrees of polymerization).

For a well-dispersed system, the aggregates of particles are small and less associated, and the viscometer spindle senses a smaller hindrance from aggregates at a given shear rate. Consequently a smaller shear stress and a lower viscosity were detected.<sup>28</sup> In contrast, the agglomerates of a poorly dispersed system forms a network that hinders the spindle and results in a higher shear stress and a higher viscosity. Figure 5 shows the apparent viscosity as a function of dispersant concentration for carbon black dispersed in water using various dispersants. For each plot, there exists a minimum in apparent viscosity. A similar trend was observed from Figures 4 and 5, which indicates that both yield value and apparent viscosity are characteristic features of a dispersed system and can evaluate the extent of dispersion in a mixture system. The results in both Figures 4 and 5 clearly indicate that stronger interactions among the dispersed particles result in a higher apparent viscosity (a higher  $\tau/\gamma$  ratio).

In Figures 4 and 5, each plot shows a minimum in apparent viscosity and yield value at 3–5 wt %. After the minimum, the apparent viscosity or yield

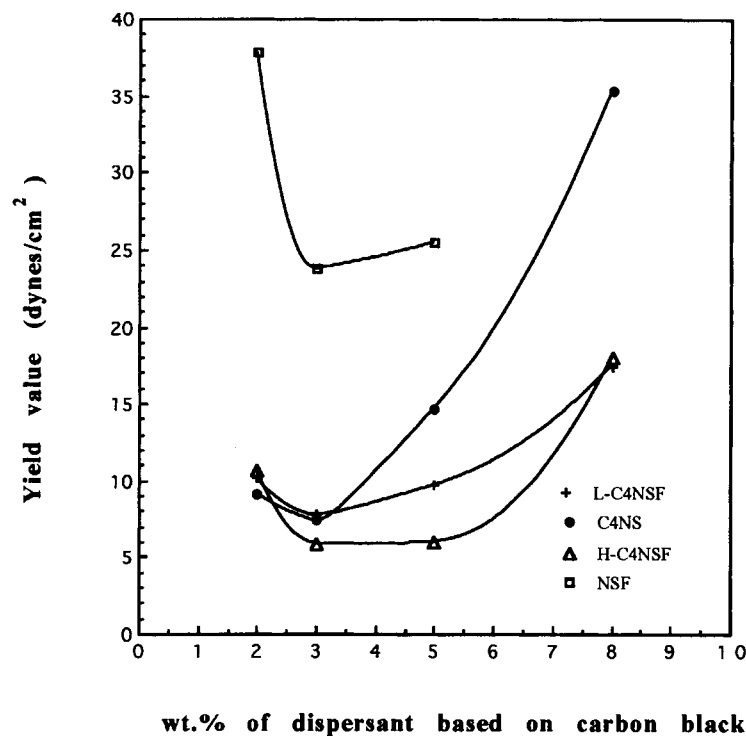
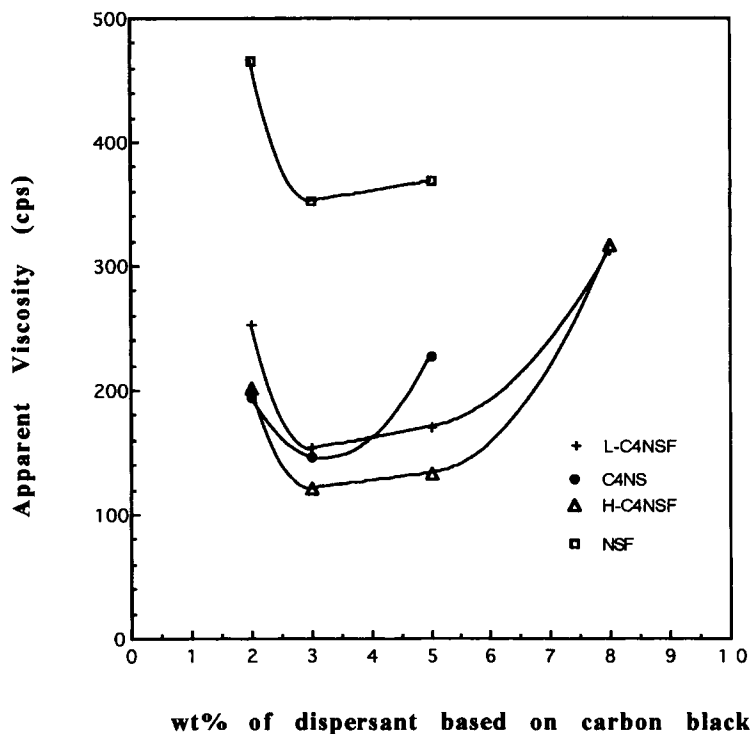


Figure 4 Yield values vs. dispersant concentration for C4NS, NSF, H-C4NSF, and L-C4NSF in the carbon black/H<sub>2</sub>O system.



**Figure 5** Apparent viscosity vs. dispersant concentration for C4NS, NSF, H-C4NSF, and L-C4NSF in the carbon black/H<sub>2</sub>O system.

value increases sharply for NSF and C4NS, but increases slowly for C4NSFs (and for C4NSFs with different molecular weight). Compared to NSF, C4NSFs show significantly lower apparent viscosity and yield values. Also C4NS shows similarly lower values compared to C4NSFs. This indicates that the substitution of a butyl group on NSF (i.e., C4NSF) or NS (i.e., C4NS) promotes their dispersing ability for carbon black in water. From Figures 4 and 5, the difference in the molecular weights of the C4NSFs synthesized in this study does not result in a significant difference in the dispersion of carbon black in water.

SEM can be used to monitor the surface of the film of dispersed particles to evaluate the dispersion state of the particles in solution. Figure 6 shows the SEM (magnification, 5000 $\times$ ) for the carbon black dispersed in water system using different concentrations of H-C4NSF [Fig. 6(a-c)] and NSF [Fig. 6(d-f)] as dispersants. For both H-C4NSF and NSF, the best dispersion occurs when the concentration is about 3 wt %. At a concentration of 3 wt %, the dispersion is better for C4NSF [Fig. 6(b)] than for NSF [Fig. 6(e)]. These results coincide with the trend observed for apparent viscosity (Fig. 5) and yield value (Fig. 4). From the comparison between Figure 6 and Figures 4–5, it is obvious that

a better dispersed system always has a lower apparent viscosity and yield value.

The effectiveness of a dispersant with specific particles is closely related to the amount adsorbed on the particles, and the properties of the dispersant at the adsorption layer. Figure 7 shows the amount adsorbed vs.  $C_{eq}^D$  (the concentration in the bulk phase at equilibrium) for C4NSF, C4NS, and NSF in the carbon black/water system. Obviously, the amount of C4NSF adsorbed is close to that of C4NS and is significantly higher than that of NSF. This result can be used to interpret the trends observed in Figures 4 and 5, where C4NSF and C4NS show a higher yield value, and a decrease in the viscosity, indicating they more efficient. The greater adsorption of C4NSF and C4NS can provide more charges on the surface of carbon black, resulting in an increase in the electrostatic repulsion, thus preventing the coagulation of the particles and a better dispersion.<sup>1,29</sup> The reason for the greater adsorption of C4NSF (or C4NS) compared to NSF can be explained by the stronger hydrophobic interactions between C4NSF (or C4NS) and the surface of carbon black due to the presence of the butyl group. Thus the butyl group in C4NSF promotes the dispersing ability of nonpolar particles, in this case carbon black in water.

In contrast to nonpolar particles, an investigation

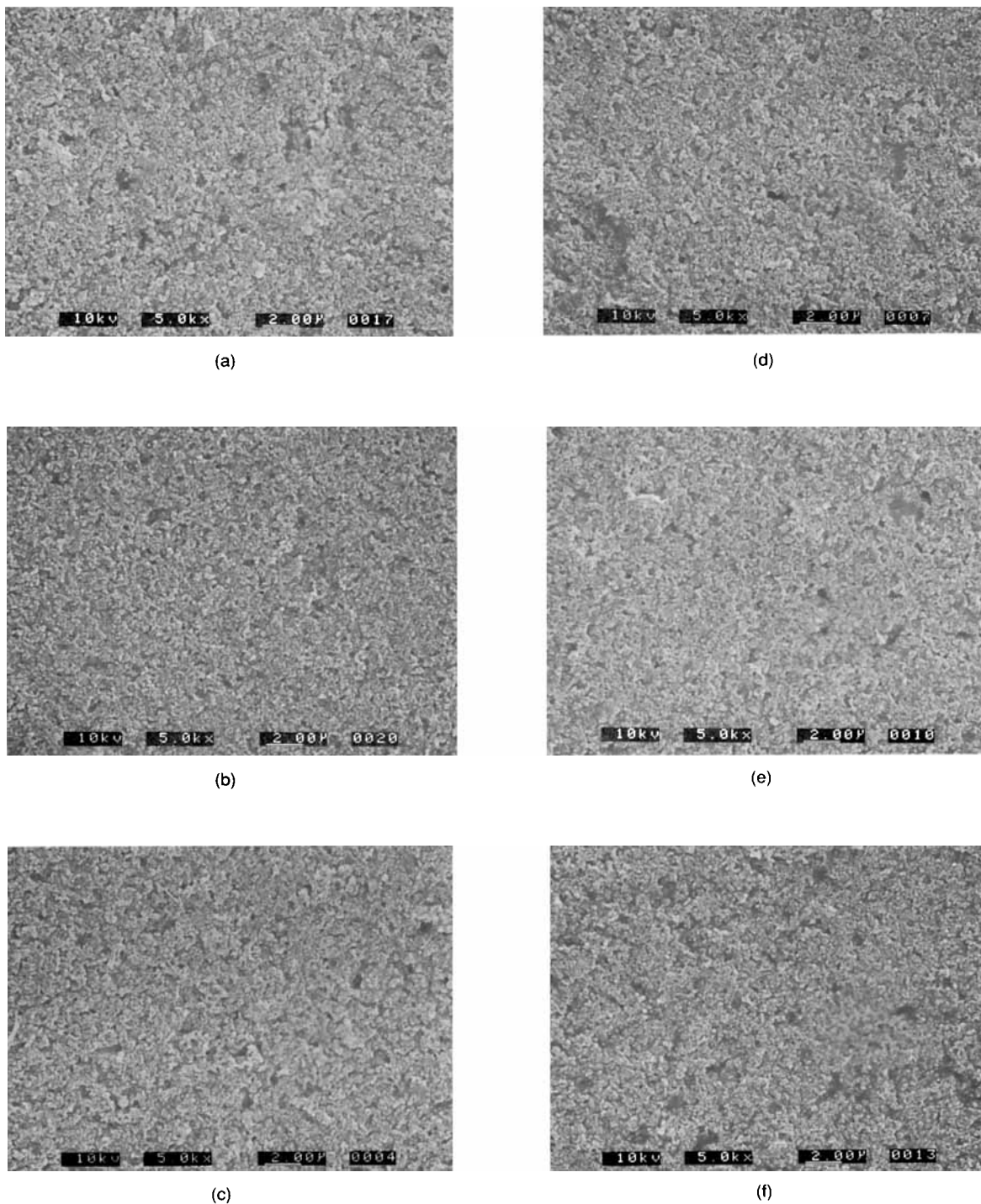


**Figure 6** The SEM (magnification 5000) for the carbon black dispersed in water using different concentrations of H-C4NSF (a, b, c) and NSF (d, e, f) as dispersants, [2 wt % based on carbon black for (a) and (d), 3 wt % for (b) and (e), and 5 wt % for (c) and (f)].

of the effect of the butyl group in C4NSF on its ability to disperse polar particles such as  $\text{TiO}_2$  was made. Figure 8 shows the apparent viscosity of  $\text{TiO}_2$  dispersed in water using C4NSF and NSF as dis-

persants as a function of dispersant concentration. The apparent viscosity of the system using C4NSF is higher than that using NSF, and it increases sharply after a concentration of about 3 wt %. The



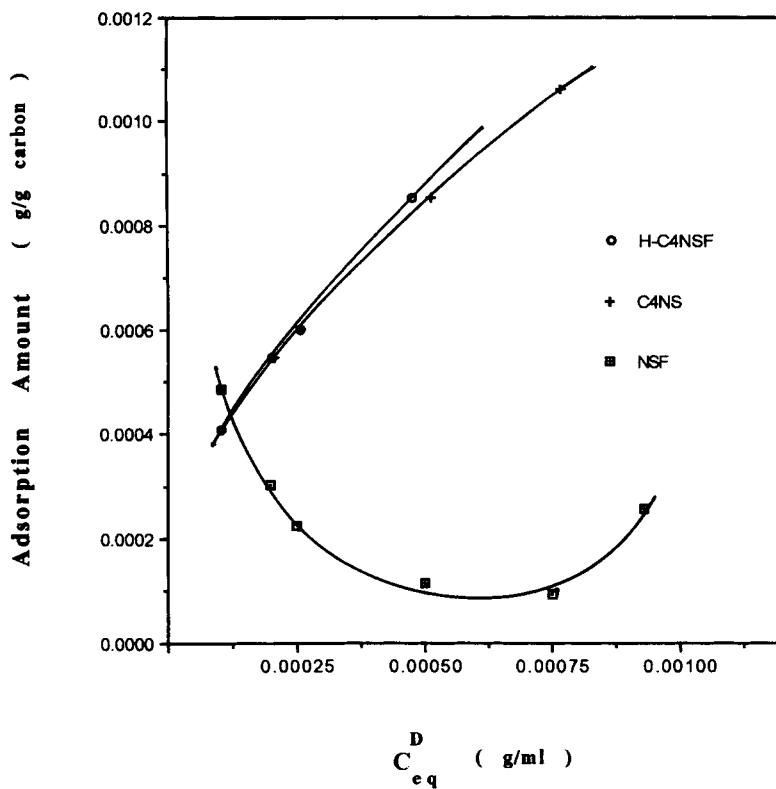


**Figure 7** The amount of C4NSF, C4NS, and NSF adsorbed on carbon black vs. the concentration in the bulk phase at equilibrium.

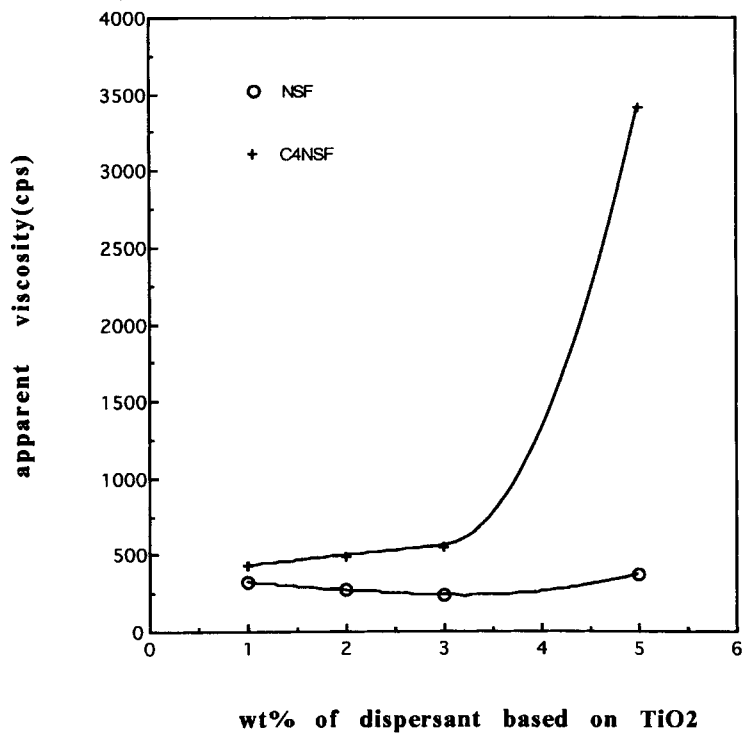


**Figure 8** Apparent viscosity vs. dispersant concentration for C4NSF and NSF in the TiO<sub>2</sub>/H<sub>2</sub>O system.

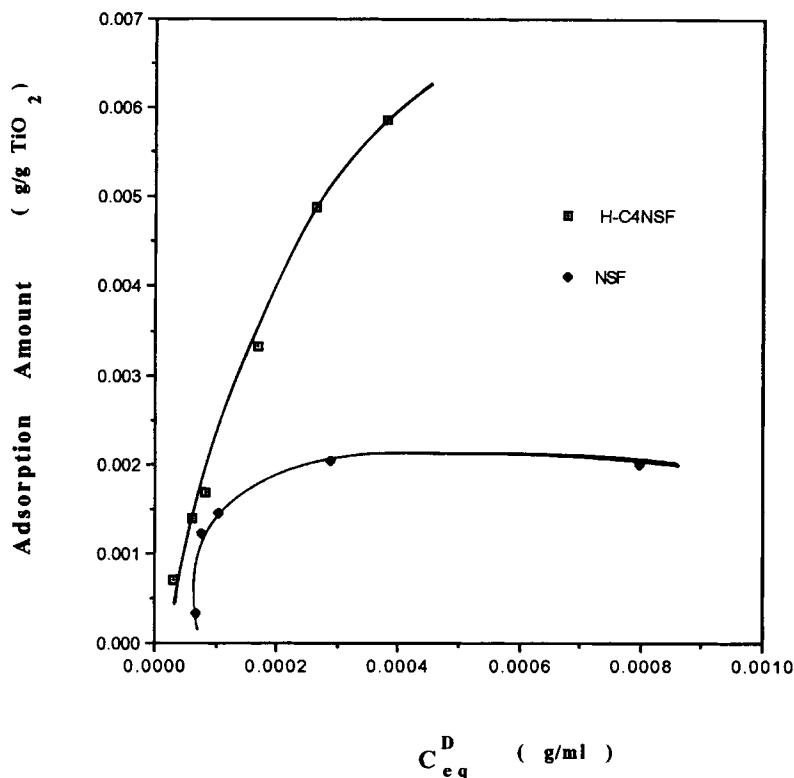


**Figure 9** The amount of C4NSF, C4NS, and NSF adsorbed on  $TiO_2$  vs. the concentration in the bulk phase at equilibrium.

sharp increase after  $\sim 3$  wt % is similar to the bridging effect observed using lipophile-grafted polycarboxylates as dispersants to disperse  $TiO_2$  in water.<sup>29,30</sup> Figure 9 shows the amount of C4NSF and NSF adsorbed on  $TiO_2$  as a function of  $C_{eq}^D$ . The amount of C4NSF adsorbed is greater than NSF. The hydrophobic interaction between adsorbed molecules is one of the mechanisms for adsorption,<sup>17,18</sup> and it enhances the adsorption. Thus, the greater adsorption of C4NSF over NSF can probably be explained by the additional hydrophobic interaction between C4NSF molecules. On the polar surface of  $TiO_2$ , the structure of C4NSF in the adsorption layer is such that the sulfonated naphthalene ring is adsorbed on the surface with the hydrophobic butyl group oriented toward the water phase.<sup>17,18</sup> Therefore, the apparent viscosity in Figure 8 can be interpreted as follows. The greater viscosity found in the C4NSF system is probably due to interactions between  $TiO_2$  particles by means of the hydrophobic interaction between adsorbed C4NSF. This causes a bridging<sup>17,18,30</sup> between the particles of  $TiO_2$  and the concomitant increase in the viscosity of the dispersed system. The sharp increase in viscosity at about 3 wt % is due to flocculation, or the so-called bridging effect.<sup>30</sup>

## CONCLUSIONS

Compared to NSF, the C4NSFs with different molecular weights show significantly lower apparent viscosities and yield values. It can be concluded that the interaction between dispersed particles such as carbon black is weaker when C4NSFs are used as dispersants than when NSF are used. This indicates that the butyl group substitution in C4NSFs promotes their dispersing ability for carbon black in water. As evidenced by microscopy of both C4NSF and NSF covered materials, the best dispersion occurs when the concentration of dispersant is 3 wt %. The dispersion is better for C4NSF than for NSF at the same concentrations. These results coincide with the trends observed for the apparent viscosity and yield value. The amount of C4NSF adsorbed onto carbon black is significantly higher than that of NSF, which explains the data in Figures 4 and 5. The higher adsorption of C4NSF provides more charges on the surface of carbon black resulting in a greater electrostatic repulsion, thus preventing the coagulation of the particles, and obtaining a better dispersion. These results indicate that the butyl group of C4NSF promotes the dispersing ability of nonpolar particles in water. The butyl group on

C4NSF affects its ability to disperse polar particles ( $\text{TiO}_2$ ), as seen in the increase in the apparent viscosity compared to NSF. The sharp increase after  $\sim 3$  wt % is similar to the bridging-effect phenomena observed using lipophile-grafted polycarboxylates as dispersants for  $\text{TiO}_2$  in water. The increased adsorption of C4NSF over NSF can be explained by the additional hydrophobic interaction between C4NSF molecules, which also causes the greater viscosity and the sharp increase with concentration observed for the  $\text{TiO}_2$ /water/C4NSF system.

The authors thank the National Science Council, Taipei, R.O.C. for their generous financial support of this research.

## REFERENCES

- G. D. Parfitt, *Dispersion of Powders in Liquids*, 3rd ed., Elsevier, New York, 1981, pp. 363, 395, 471.
- P. Swaraj, *Surface Coatings Science and Technology*, Wiley, New York, 1985, pp. 381, 558.
- T. C. Patton, *Paint Flow and Pigment Dispersant*, 2nd ed., Wiley, New York, 1979, p. 273.
- F. P. Henry, *Organic Coating Technology*, Vol. 2, Wiley, New York, 1970, p. 675.
- R. L. Graut, *Paper Technol.*, **3**, 539 (1962).
- J. W. Gooch, *J. Coatings Technol.*, **60**, 37 (1988).
- J. H. Hunter, *Foundations of Colloid Science*, Vol. 1, Clarendon Press, 1987, p. 89.
- D. H. Solomon and D. C. Hawthorne, *Chemistry of Pigment and Fillers*, Wiley, New York, 1983, p. 118.
- W. H. Berggren and W. W. Swanson, *Additive Development for Ultraclean Coal Slurry Fuel*, AMAX Research & Development Center, 1988.
- D. M. Roy and K. Asaga, *Chem. Concr. Res.*, **9**, 731 (1979).
- J. E. Funk, U. S. Pat. 88,815 (1979).
- A. Pierre, J. M. Lamarche, R. Mercieer, and A. Foissy, *Chem. Concr. Res.*, **19**, 692 (1989).
- K. Hattori, *Nippon Nogei Kagaku Kaishi*, **52**, R127-R137 (1978).
- K. Hattori, C. Yamakawa, S. Suzue, T. Azuma, T. Imamura, and Y. Ejiri, *Rev. Gen. Meet., Tech. Sess.—Chem. Assoc. Jpn.*, Tokyo, Japan, 1976, pp. 30, 153.
- K. Hattori and Y. Tanino, *Kogyo Kagaku Zasshi*, **66**, 55 (1963).
- E. K. Raymond and F. O. Donald, *Encyclopedia of Chemical Technology*, 3rd ed., Vol. 22, Wiley, New York, 1983, p. 1.
- M. J. Rosen, *Surfactants and Interfacial Phenomena*, Wiley, New York, 1978, p. 252.
- Ibid.*, p. 32.
- C. J. Pouchert, *The Aldrich Library of NMR Spectra*, 2nd ed., Vol. 2, Aldrich Chemical Company, Inc., Milwaukee, Wisconsin, 1983.
- Q. T. Pham, R. P. Tiaud, Marie-France Llauro, and Hugues Waton, *Proton and Carbon NMR Spectra of Polymer*, Wiley, New York, 1984.
- J. F. Rabek, *Experimental Methods in Polymer Chemistry*, Wiley, New York, 1980, p. 419.
- D. M. Roy, G. Varadi, F. D. Tamas, G. Palyi, and B. Bartha, *Chem. Concr. Res.*, **14**, 439 (1984).
- M. J. Garvey, Th. F. Tadros, *Kolloid-Z.u.z. Polymer*, **250**, 967 (1972).
- K. Hattori and Y. Tanino, *Kogyo Kagaku Zasshi*, **67**, 1401 (1964).
- S. L. Rosen, *Fundamental Principles of Polymeric Materials*, Wiley, 1982, pp. 88, 281.
- Tatsuo Sato, *J. Coatings Technol.*, **51**, 657 (1979).
- P. E. Pierce, *J. Paint Technol.*, **43**, 21 (1982).
- M. Noboru, *Bull. Chem. Soc. Jpn.*, **48**, 1713 (1975).
- P.-L. Kuo, T.-C. Chang, L.-M. Lu, *J. Appl. Polym. Sci.*, **44**, 859 (1992).
- P.-L. Kuo, T.-C. Chang, *J. Appl. Polym. Sci.*, **44**, 869 (1992).
- P.-L. Kuo, S.-C. Ni, C.-C. Lai, *J. Appl. Polym. Sci.*, **45**, 611 (1992).

Received January 20, 1992

Accepted March 20, 1992